

CONTROL OF STAR FORMATION IN GALAXIES BY GRAVITATIONAL INSTABILITY

YUEXING LI, MORDECAI-MARK MAC LOW

Department of Astronomy, Columbia University, New York, NY 10027, USA and
Department of Astrophysics, American Museum of Natural History, New York, NY 10024, USA

AND

RALF S. KLESSEN

Astrophysikalisches Institut Potsdam, An der Sternwarte 16, D-14482 Potsdam, Germany
Draft version November 21, 2018

ABSTRACT

We study gravitational instability and consequent star formation in a wide range of isolated disk galaxies, using three-dimensional, smoothed particle hydrodynamics simulations at resolution sufficient to fully resolve gravitational collapse. Stellar feedback is represented by an isothermal equation of state. Absorbing sink particles are inserted in dynamically bound, converging regions with number density $n > 10^3 \text{ cm}^{-3}$ to directly measure the mass of gravitationally collapsing gas available for star formation. Our models quantitatively reproduce not only the observed Schmidt law, but also the observed star formation threshold in disk galaxies. Our results suggest that the dominant physical mechanism determining the star formation rate is just the strength of gravitational instability, with feedback primarily functioning to maintain a roughly constant effective sound speed.

Subject headings: galaxy: evolution — galaxy: spiral — galaxy: star clusters — stars: formation

1. INTRODUCTION

Stars form in galaxies at hugely varying rates (Kennicutt 1998a). The mechanisms that control the star formation rate from interstellar gas are widely debated (Shu, Adams & Lizano 1987; Elmegreen 2002; Larson 2003; Mac Low & Klessen 2004). Gravitational collapse is opposed by gas pressure, supersonic turbulence, magnetic fields, and rotational shear. Gas pressure in turn is regulated by radiative cooling and stellar and turbulent heating. Despite this complexity, star-forming spiral galaxies follow two empirical laws. First, stars only form above a critical gas surface density (Martin & Kennicutt 2001) that appears to be determined by the Toomre (1964) criterion for gravitational instability. Second, the rate of star formation is proportional to a power of the total gas surface density (Schmidt 1959; Kennicutt 1998b).

A number of groups have simulated disk galaxies in isolation or in mergers, or in cosmological contexts, e.g., Mihos & Hernquist (1994); Friedli & Benz (1995); Sommer-Larsen, Gelato & Vedel (1999); Springel (2000); Barnes (2002); Governato et al. (2004). Robertson et al. (2004) review this work. However, in these simulations, star formation is generally set up with empirical recipes *a priori*. The origin of the observed Schmidt law remains unclear.

Recent cosmological simulations with moderate mass resolution by Kravtsov (2003) show that the Schmidt law is a manifestation of the overall density distribution of the ISM, and find little contribution from feedback. However, the strength of gravitational instability was not directly measured in his work, so a direct connection could not be made between instability and the Schmidt Law, as we do here. The importance of gravitational instability in controlling large-scale star formation was emphasized by Friedli & Benz (1995) and Elmegreen (2002). A simi-

lar conclusion comes from the observation that thin dust lanes in galaxies only form in gravitationally unstable regions (Dalcanton, Yoachim & Bernstein 2004).

We simulate a large set of isolated galaxies to investigate gravitational instability and consequent star formation. In this Letter, we examine star formation as a function of gravitational instability, and compare the global Schmidt law and star formation thresholds derived from our simulations to the observations.

2. COMPUTATIONAL METHOD

We use the smoothed particle hydrodynamics (SPH) code GADGET (Springel, Yoshida & White 2001), modified to include absorbing sink particles (Bate, Bonnell & Price 1995) to directly measure the mass of gravitationally collapsing gas. Sink particles, representing star clusters (SCs), replace gravitationally bound regions of converging flow that reach number densities $n > 10^3 \text{ cm}^{-3}$. (These regions have pressures $P/k \sim 10^7 \text{ K cm}^{-3}$ typical of star-forming regions.)

Our galaxy model consists of a dark matter halo, and a disk of stars and isothermal gas. The galaxy structure is based on the analytical work by Mo, Mao & White (1998), as implemented numerically by Springel & White (1999) and Springel (2000). The isothermal sound speed is chosen to be either $c_1 = 6 \text{ km s}^{-1}$ in models with low temperature T or $c_2 = 15 \text{ km s}^{-1}$ in high T models. Table 1 lists the most important model parameters. The Toomre criterion for gravitational instability that couples stars and gas, Q_{sg} is calculated following Rafikov (2001), and the minimum value is derived using the wavenumber k of greatest instability and lowest Q_{sg} at each radius.

The gas, halo and disk particles are distributed with number ratio $N_{\text{g}} : N_{\text{h}} : N_{\text{d}} = 5 : 3 : 2$. The gravitational softening lengths of the halo $\epsilon_{\text{h}} = 0.4 \text{ kpc}$ and disk $\epsilon_{\text{d}} = 0.1 \text{ kpc}$, while that of the gas ϵ_{g} is given in Table 1 for each model. The minimum spatial and mass resolutions in the gas are given by ϵ_{g} and twice

TABLE 1
GALAXY MODELS AND NUMERICAL PARAMETERS

Model ^a	f_g ^b	$Q_{sg}(LT)$ ^c	$Q_{sg}(HT)$ ^d	N_{tot} ^e	ϵ_g ^f	m_g ^g
G50-1	1	1.22	1.45	1.0	10	0.08
G50-2	2.5	0.94	1.53	1.0	10	0.21
G50-3	4.5	0.65	1.52	1.0	10	0.37
G50-4	9	0.33	0.82	1.0	10	0.75
G100-1	1	1.08	...	6.4	7	0.10
G100-1	1	...	1.27	1.0	10	0.66
G100-2	2.5	...	1.07	1.0	10	1.65
G100-3	4.5	...	0.82	1.0	10	2.97
G100-4	9	...	0.42	1.0	20	5.94
G120-3	4.5	...	0.68	1.0	20	5.17
G120-4	9	...	0.35	1.0	30	10.3
G160-1	1	...	1.34	1.0	20	2.72
G160-2	2.5	...	0.89	1.0	20	6.80
G160-3	4.5	...	0.52	1.0	30	12.2
G160-4	9	...	0.26	1.5	40	16.3
G220-1	1	0.65	...	6.4	15	1.11
G220-1	1	...	1.11	1.0	20	7.07
G220-2	2.5	...	0.66	1.2	30	14.8
G220-3	4.5	...	0.38	2.0	40	15.9
G220-4	9	...	0.19	4.0	40	16.0

^aFirst number is rotational velocity in km s^{-1} at virial radius.

^bPercentage of total halo mass in gas.

^cMinimum initial Q_{sg} for low T model. Missing data indicates models not run at full resolution.

^dMinimum initial Q_{sg} for high T model

^eMillions of particles in high resolution runs.

^fGravitational softening length of gas in pc.

^gGas particle mass in units of $10^4 M_\odot$.

the kernel mass ($\sim 80m_g$). We adopt typical values for the halo concentration parameter $c = 5$, spin parameter $\lambda = 0.05$, and Hubble constant $H_0 = 70 \text{ km s}^{-1} \text{ Mpc}^{-1}$ (Springel 2000). The spin parameter used is a typical one for galaxies subject to the tidal forces of the cosmological background. Reed et al. (2003) suggest a wide range of c for galaxy-size halos. However, this parameter is based on a simple model of the halo formation time (Navarro, Frenk & White 1997), with poorly known distribution (Mo et al. 1998). Springel & White (1999) suggest that $c = 5$ is theoretically expected for flat, low-density universes.

Models of gravitational collapse must satisfy three numerical criteria: the Jeans resolution criterion (Bate & Burkert 1997, hereafter BB97; Whitworth 1998), the gravity-hydro balance criterion for gravitational softening (BB97), and the equipartition criterion for particle masses (Steinmetz & White 1997). Truelove et al. (1998) suggest that a Jeans mass must be resolved with far more than the $N_k = 2$ smoothing kernels proposed by BB97. Therefore we performed a resolution study of model G100-1 (LT) with $N_{tot} = 10^5$, 8×10^5 , and 6.4×10^6 , corresponding to $N_k \approx 0.4$, 3.0 and 23.9, respectively. We find convergence to within 10% of the global amount of mass accreted by sink particles between the two highest resolutions, suggesting that the BB97 criterion is sufficient for the problem considered here.

We performed 24 simulations satisfying all three criteria, including six models of low mass galaxies with low T to study the effect of changing the effective sound speed. We also set a minimum value of $N_{tot} \geq 10^6$ particles for

lower mass galaxies resolved with fewer particles.

3. GLOBAL SCHMIDT LAW

To derive the Schmidt law, we average Σ_{SFR} and Σ_{gas} over the star forming region following Kennicutt (1989), with radius chosen to encircle 80% of the mass in sinks. To estimate the star formation rate, we make the assumption that individual sinks represent dense molecular clouds that form stars at some efficiency. Observations by Rownd & Young (1999) suggest that the *local* star formation efficiency (SFE) in molecular clouds remains roughly constant. Kennicutt (1998b) shows a median SFE of 30% in starburst galaxies dominated by molecular gas. This suggests the local SFE of dense molecular clouds around 30%. We therefore adopt a fixed local SFE of $\epsilon = 30\%$ to convert the mass of sinks to stars. Note that this local efficiency is different from the global star formation efficiency in galaxies, which measures the fraction of the *total* gas turned into stars. The global SFE can range from 1–100% (Kennicutt 1998b), depending on the gas distribution and the molecular gas fraction.

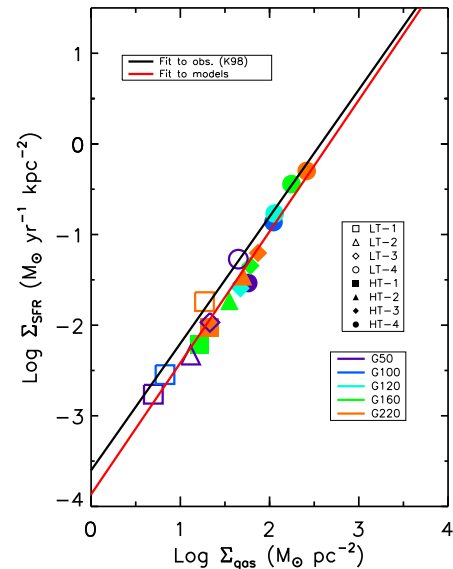


FIG. 1.— Schmidt law from fully resolved low (*open symbols*) and high (*filled symbols*) T models listed in Table 1 that showed gravitational collapse. The colors indicate the galaxy rotational velocities, while the symbol shapes indicate the gas fractions, as specified in the legend. The black line is the best fit to the observations from Kennicutt (1998b), while the red line is the best fit to the simulations.

Figure 1 shows the Schmidt law derived from our simulations. The best fit to the observations by Kennicutt (1998b) gives a Schmidt law $\Sigma_{SFR} = A \Sigma_{gas}^\alpha$ with global efficiency $A = (2.5 \pm 0.7) \times 10^{-4}$ and power law $\alpha = 1.4 \pm 0.15$, where Σ_{SFR} is given in units of $M_\odot \text{ kpc}^{-2} \text{ yr}^{-1}$, and Σ_{gas} is given in units of $M_\odot \text{ pc}^{-2}$. A least-squares fit to the models listed in Table 1 (both low T and high T) gives $A = (1.4 \pm 0.4) \times 10^{-4}$ and $\alpha = 1.45 \pm 0.07$, agreeing with the observations to within the errors.

Note LT models tend to have slightly higher SF rates than equivalent HT models. Thus, observations may be able to directly measure the effective sound speed

(roughly equivalent to velocity dispersion) of the star-forming gas in galactic disks and nuclei. More simulations will be needed to demonstrate this quantitatively.

Our chosen models do not populate the lowest and highest star formation rates observed. Interacting galaxies can produce very unstable disks and trigger vigorous starbursts (e.g., Li, Mac Low & Klessen 2004). Quiescent normal galaxies form stars at a rate below our mass resolution limit. Our most stable models indeed show no star formation in the first few billion years.

4. STAR FORMATION THRESHOLD

A threshold is clearly visible in the spatial distribution of gas and stars in our galaxy models, as illustrated in Figure 2. The critical value of the instability parameter at threshold can be quantitatively measured from the radial profile as indicated in the middle panel, which shows a sharp drop of Σ_{SFR} at $R \sim 2R_{\text{d}}$. The critical values of Q_{sg} and Q_{g} at the threshold R_{th} are shown in the bottom panel of Figure 2 for all the fully resolved models listed in Table 1. The critical values of Q_{sg} appear to be generally higher than Q_{g} in the same galaxy, and both have lower values (< 1) in more unstable models.

Most galaxies not classified as starbursts have gas fractions comparable to or less than our most stable models, so the observation of a threshold value of $Q_{\text{g}} \sim 1.4$ may reflect the stability of the galaxies in the sample (Martin & Kennicutt 2001). Observed variations in the threshold also appear to occur naturally. If we only use the Toomre criterion for the gas Q_{g} we get slightly larger scatter than if we include the stars and use the combined criterion Q_{sg} , but the effect is small.

5. DISCUSSION AND SUMMARY

What controls star formation in different galaxies? Our models suggest the answer is the nonlinear development of gravitational instability. Figure 3 shows the correlation between the star formation timescale τ_{SF} and the initial minimum $Q_{\text{sg}}(\text{min})$ for fully resolved models listed in Table 1. The best fit is $\tau_{\text{SF}} = (34 \pm 7 \text{ Myr}) \times \exp[(4.2 \pm 0.3)Q_{\text{sg}}(\text{min})]$. Quiescent star formation occurs where Q_{sg} is large, while vigorous starbursts occur where Q_{sg} is small. This differs from the emphasis on supersonic turbulence by Kravtsov (2003). The maximum strength of instability $Q_{\text{sg}}(\text{min})$ depends on the mass of the galaxy and the gas fraction. The larger the halo mass, or the larger the gas fraction, the smaller resulting $Q_{\text{sg}}(\text{min})$, and thus the shorter τ_{SF} .

Typical observed starburst times of 10^8 yr are consistent with our fit for τ_{SF} (Kennicutt 1998b). This also agrees with the observations by MacArthur et al. (2004) that the star formation rate depends on the galaxy potential. McGaugh et al. (2000) show a break in the Tully-Fisher relation for galaxies with $V_{\text{c}} \leq 90 \text{ km s}^{-1}$, suggesting a transition at this scale. Indeed, our models with $V_{\text{c}} \leq 100 \text{ km s}^{-1}$ and gas fraction $\leq 50\%$ of the disk mass appear to be rather stable ($Q_{\text{sg}} > 1.0$), with no star formation in the first 3 Gyrs, while models with $V_{\text{c}} \geq 120 \text{ km s}^{-1}$ become less stable, forming stars easily. This is also consistent with the rotational velocity above which dust lanes are observed to form (Dalcanton et al. 2004).

We have deferred inclusion of explicit feedback, magnetic fields, and gas recycling to future work. However,

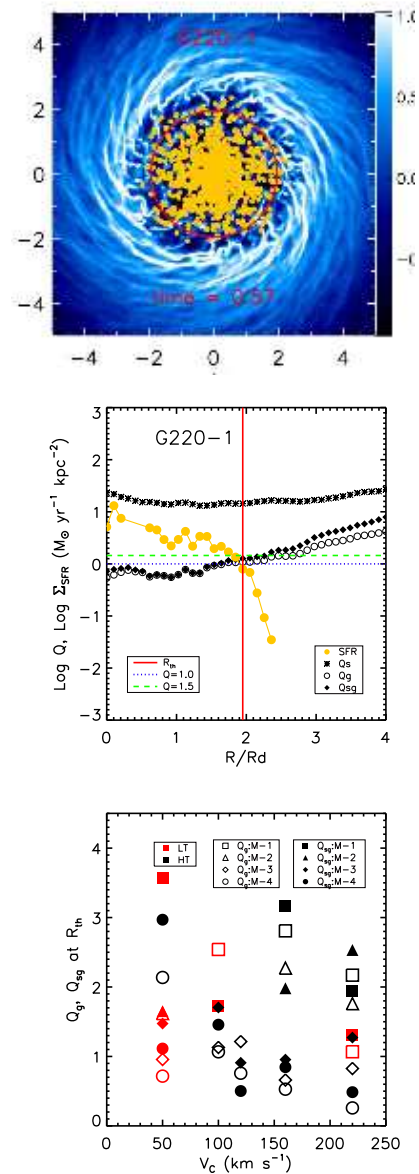


Fig. 2.— (Top) Star formation threshold illustrated by the low T model G220-1 with $N_{\text{tot}} = 6.4 \times 10^6$. Log of gas surface density is shown, with values given by the color bar. Yellow dots indicate SCs, while the red circle shows R_{th} . (Middle) Radial profiles of star formation rate (yellow circles), and Toomre Q parameters for stars Q_{s} (asterisks), gas Q_{g} (circles), and stars and gas combined Q_{sg} (diamonds). The red line shows R_{th} . Bottom: critical values of Q_{sg} (filled symbols) and Q_{g} (open symbols) at R_{th} for both low (red) and high (black) T models.

we believe each will have minor effects on the questions considered here. The assumption of an isothermal equation of state for the gas implies substantial feedback to maintain the effective temperature of the gas against radiative cooling and turbulent dissipation. Real interstellar gas has a wide range of temperatures. However, the rms velocity dispersion generally falls within the range $6\text{--}12 \text{ km s}^{-1}$ (e.g., Elmegreen & Scalo 2004). Direct feedback from starbursts may play only a minor role in quenching subsequent star formation

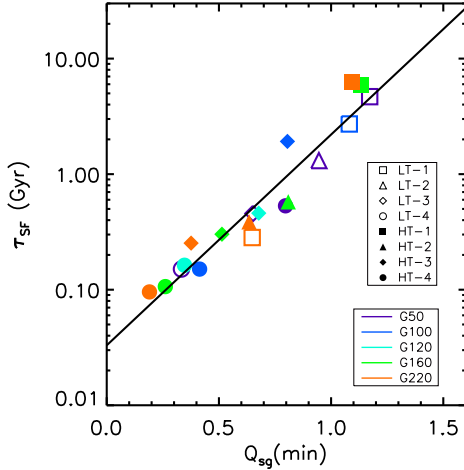


FIG. 3.— Star formation timescale τ_{SF} as a function of initial $Q_{\text{sg}}(\text{min})$, for both low T (open symbols) and high T (filled symbols) models. The solid line is the least-square fit.

(e.g., Kravtsov 2003; Monaco 2004), perhaps because most energy is deposited not in the disk but above it as superbubbles blow out (e.g., Fujita et al. 2003; Avillez & Breitschwerdt 2004). Kim & Ostriker (2001) demonstrate that swing and magneto-Jeans instabilities operating in a gaseous disk occur at $Q_g \sim 1.4$, suggesting that magnetostatic support is unimportant. The lack of gas recycling both from disrupted molecular clouds and from massive stars will change the detailed patterns of star formation, but probably not the overall results.

Simulations of isolated, isothermal disks by Robertson et al. (2004) show large-scale collapse in their centers leading to disks far smaller than observed, which they argued was caused by an isothermal equation of state. This behavior does not occur in our model with physical parameters close to theirs, but resolution sufficient to resolve the Jeans length. Similarly,

Governato et al. (2004) argue that several long-standing problems in galaxy simulations such as the angular momentum catastrophe may well be caused by inadequate resolution, or violation of the other numerical criteria. We will present more resolution studies in future work.

In summary, our models reproduce quantitatively not only the Schmidt law, but also the star formation threshold in disk galaxies. We find a direct correlation between the star formation rate and the strength of gravitational instability. This suggests that gravitational instability in effectively isothermal gas may be the dominant physical mechanism that controls the rate and location of star formation in galaxies. Unstable galaxies were more common at early cosmic times, so our results, together with merger-induced starbursts (Li et al. 2004) may account for the Butcher-Oemler effect (Butcher & Oemler 1984) of increasing blueness of galaxies with redshift. Massive galaxies form stars quickly, which may account for the downsizing effect that star formation first occurs in big galaxies at high redshift, while modern starburst galaxies are small (Cowie et al. 1996; Poggianti et al. 2004; Ferreras et al. 2004). The slow evolution of star formation in our low mass models resembles that observed in low surface brightness galaxies (van den Hoek et al. 2000).

We thank V. Springel for making both GADGET and his galaxy initial condition generator available, as well as for useful discussions, A.-K. Jappsen for participating in the implementation of sink particles in GADGET, and F. Adams, J. Dalcanton, R. Kennicutt, J. Lee, C. Martin, D. McCray, T. Quinn, M. Shara, and J. van Gorkom for useful discussions. The referee, F. Governato, also gave valuable comments. This work was supported by NSF grants AST99-85392 and AST03-07854, NASA grant NAG5-13028, and DFG Emmy Noether grant KL1358/1. Computations were performed at the Pittsburgh Supercomputer Center supported by the NSF, on the Parallel Computing Facility of the AMNH, and on an Ultrasparc III cluster generously donated by Sun Microsystems.

REFERENCES

- Avillez, M. A., & Breitschwerdt, D. A&A 425, 899
 Barnes, J. E. 2002 MNRAS 333, 481
 Bate, M. R., Bonnell, I. A., & Price, N. M. 1995 MNRAS 277, 362
 Bate, M. R. & Burkert, A. 1997 MNRAS 288, 1997
 Butcher, H. & Oemler, A. Jr. 1984 ApJ 285, 426
 Cowie, L. L., Songaila, A., Hu, E. M. & Cohen, J. G. 1996 AJ 112, 839
 Dalcanton, J., Yoachim, P. & Bernstein, R. A. 2004 ApJ 608, 189
 Elmegreen, B. G. 2002 ApJ 577, 206
 Elmegreen, B. G., & Scalo, J. 2004 ARAA 42, 275
 Ferreras, I., Silk, J., Böhm, A. & Ziegler, B. 2004 MNRAS 355, 64
 Friedli, D. & Benz, W. 1995 A&A 301, 649
 Fujita, A., Martin, C. L., Mac Low, M.-M. & Abel, T. 2003 ApJ 599, 50
 Governato, F. et al. 2004 ApJ 607, 688
 Kennicutt, R. C., Jr. 1989, ApJ 344, 685
 Kennicutt, R. C., Jr. 1998, ARA&A 36, 189
 Kennicutt, R. C., Jr. 1998, ApJ 498, 541
 Kim, W.-T., & Ostriker, E. C. 2001 ApJ 559, 70
 Kravtsov, A. V. 2003 ApJL 590, 1
 Larson, R. B. 2003 Rep. Prog. Phys. 66, 1651
 Li, Y., Mac Low, M.-M. & Klessen, R. S. 2004 ApJL, 614, 29
 MacArthur, L. A., Courteau, S, Bell, E. & Holtzman, J. A. 2004 ApJS 152, 175
 McGaugh, S. S.; Schombert, J. M.; Bothun, G. D. & de Blok, W. J. G. 2000 ApJ 533, 99
 Mac Low, M.-M. & Klessen, R. S. 2004 Rev. Mod. Phys. 76, 125
 Martin, C. L. & Kennicutt, R. C. Jr. 2001 ApJ 555, 301
 Mihos, C.J. & Hernquist, L. 1994 ApJL 431, 9
 Mo, H. J., Mao, S., & White, S. D. M. 1998 MNRAS 295, 319
 Monaco, P. 2004 MNRAS 352, 181
 Navarro, J. F., Frenk, C. S., & White, S. D. M. 1997 ApJ 487, 73
 Poggianti, B. M. et al. 2004 ApJ 601, 197
 Rafikov, R. R. 2001 MNRAS 323, 2001
 Reed, D. et al. 2003 preprint, astro-ph/0312544
 Robertson, B., Yoshida, N., Springel, V. & Hernquist, L. 2004 ApJ 606, 32
 Rownd, B. K., & Young, J. S. 1999 AJ 118, 670
 Schmidt, M. 1959 ApJ 129, 243
 Shu, F., Adams, F. C. & Lizano, S. 1987 ARA&A 25, 23
 Sommer-Larsen, J., Gelato, S., & Vedel, H. 1999 ApJ 519, 501
 Springel, V. 2000 MNRAS 312, 859
 Springel, V. & White, S. M. D. 1999 MNRAS 307, 162
 Springel, V., Yoshida, N. & White, S. D. M. New Astron. 6, 79
 Steinmetz, M. & White, S. D. M. 1997 MNRAS 288, 545
 Toomre, A. 1964 ApJ 139, 1217
 Truelove J. K. et al. 1998 ApJ 495, 821
 van den Hoek, L. B., de Blok, W. J. G., van der Hulst, J. M. & de Jong, T. 2000 ApJ 357, 397

Whitworth, A. P. 1998 MNRAS 296, 442